AD-A160 326 TURBULENT NONCONDENSING AND CONDENSING GAS JETS IN LIQUIDS(U) PENNSYLVANIA STATE UNIV UNIVERSITY PARK DEPT OF MECHANICAL ENGINEERING T Y SUN ET AL. AUG 85 1/1

UNCLASSIFIED N00014-85-K-0148 F/G 20/4 NL

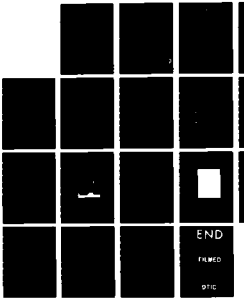

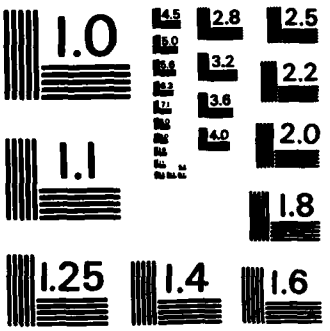

(12)

Final Report

TURBULENT NONCONDENSING AND CONDENSING GAS JETS IN LIQUIDS

by

T.-Y. Sun, S.G. Chuech, R.N. Parthasarathy and G.M. Faeth
Department of Mechanical Engineering
The Pennsylvania State University
University Park, Pennsylvania 16802

Prepared for:

Department of the Navy
Office of Naval Research
Propulsion and Energetics (Code 432P)
800 N. Quincy Street
Arlington, Virginia 22217-5000

Contract No. N00014-85-K-0148
M.K. Ellingsworth
Scientific Program Officer

August 1985
Report No. N00014-85-K-0148-1985

Unclassified

SECURITY CLASSIFICATION OF THIS PAGE (When Data Entered)

REPORT DOCUMENTATION PAGE	READ INSTRUCTIONS BEFORE COMPLETING FORM
1. REPORT NUMBER: N00014-85-K-0148-1985	2. GOVT ACCESSION NO.: AD-A160336
	3. RECIPIENT'S CATALOG NUMBER:
4. TITLE (and Subtitle): Turbulent Noncondensing and Condensing Gas Jets in Liquids	5. TYPE OF REPORT & PERIOD COVERED: Final Report 12/15/84 to 7/31/85
	6. PERFORMING ORG. REPORT NUMBER:
7. AUTHOR(s): T.-Y. Sun, S.G. Chuech, R.N. Parthasarathy and G.M. Faeth	8. CONTRACT OR GRANT NUMBER(s): N00014-85-K-0148
9. PERFORMING ORGANIZATION NAME AND ADDRESS: Department of Mechanical Engineering, The Pennsylvania State University, University Park, PA 16802	10. PROGRAM ELEMENT, PROJECT, TASK AREA & WORK UNIT NUMBERS:
11. CONTROLLING OFFICE NAME AND ADDRESS: Office of Naval Research, 800 North Quincy Street, Arlington, VA 22217	12. REPORT DATE: August, 1985
	13. NUMBER OF PAGES: 35
14. MONITORING AGENCY NAME & ADDRESS(if different from Controlling Office):	15. SECURITY CLASS. (of this report): Unclassified
	15a. DECLASSIFICATION/DOWNGRADING SCHEDULE:

16. DISTRIBUTION STATEMENT (of this Report)

Approved for public release; distribution unlimited.

17. DISTRIBUTION STATEMENT (of the abstract entered in Block 20, if different from Report)

18. SUPPLEMENTARY NOTES

19. KEY WORDS (Continue on reverse side if necessary and identify by block number)

Multiphase flow, gas jets in liquids, exhaust plumes, compressible turbulent jets.

20. ABSTRACT (Continue on reverse side if necessary and identify by block number)

Research concerning gas injection into liquids is reported. This flow is important, since it is a fundamental multiphase flow, analagous to the round jet for single-phase flows. The flow also has several direct applications, e.g., stored chemical energy propulsion systems (SCEPS), direct-contact condensers, gas dissolution systems, reservoir destratification systems and nuclear-reactor pressure suppression systems. Stability of these flows is enhanced when an underexpanded jet is used; therefore, the interaction of supersonic wave structures with liquids in turbulent flow

DD FORM 1 JAN 73 1473 EDITION OF 1 NOV 65 IS OBSOLETE

S/N 0102-LF-014-6601

SECURITY CLASSIFICATION OF THIS PAGE (When Data Entered)

cont

is also an issue.

The objective of this ~~short initial~~ phase of the study was to develop test apparatus relating to underexpanded air jets in air (which is a baseline for subsequent work) and turbulent subsonic gas jets in liquids. The ~~air-jet-in-air~~ apparatus was assembled and ~~initial~~ flow visualization tests were completed using continuous and spark Schlieren photography. Operation of the apparatus was satisfactory and data has been accumulated on the geometry of the Mach disk which forms at higher levels of underexpansion. Analysis of turbulent subsonic flow properties has also been implemented. Subsequent measurements will include mean and fluctuating velocities, using laser Doppler anemometry; mean and fluctuating density, using Rayleigh scattering; and mean and fluctuating concentrations, using laser-induced fluorescence. Subsequent analysis will involve extension to include underexpanded jet conditions and the supersonic wave structure.

Test apparatus for gas injection in liquids was assembled. Tests were also undertaken ~~in a subscale apparatus~~ to study injector stability. Test results showed that jet instability for subsonic (adapted) flow could be controlled by placing a screen across the jet exit and controlling gas release at the surface of the bath (which can cause undesirable pressure fluctuations in the bath). For stable jets, the liquid/gas interface is continuous near the jet exit and its position is influenced by the degree of underexpansion. A bubble cloud was observed near the interface, it is also probable that a drop cloud is present as well. Analysis of this flow for subsonic jet exit conditions was implemented using the locally homogeneous flow approximation of multiphase flow. The next phase of the work will involve measurements of mean and fluctuating velocities, using laser Doppler anemometry, for a water jet (as a baseline); and void fraction distribution for gas injection in liquids, using gamma-ray absorption.

Keywords: Exhaust plumes, Compressible turbulent jets

ACKNOWLEDGEMENTS

The authors acknowledge the assistance of Roger Glass, Clete Iott, Warren Eaton and Thomas Griffin for their help in setting up test apparatus in the Gas Dynamics Laboratories of the University of Michigan. We also thank Clete Iott for valuable technical assistance in assembling and operating the Schlieren apparatus.

TABLE OF CONTENTS

LIST OF TABLES

LIST OF FIGURES

NOMENCLATURE

Symbol	Description
a	acceleration of gravity
C_i	constants in turbulence model
d	injector exit diameter
f	mixture fraction
g	square of mixture fraction fluctuations
k	turbulent kinetic energy
$P(f),P(f)$	time-averaged probability density functions of f, Favre-averaged probability density function of f
r	radial distance
Re	injector Reynolds number
S_ϕ	source term
u	axial velocity
v	radial velocity
x	height above injector
ε	rate of dissipation of turbulence kinetic energy
μ_t	turbulent viscosity
ρ	density
σ_i	turbulent Prandtl/Schmidt number
ϕ	generic property

Subscripts

c	centerline value
o	burner exit condition
∞	ambient condition

Superscripts

$\bar{(\,)}$	time-averaged quantity
$\tilde{(\,)}$	Favre-averaged quantity
$(\,)',\bar{(\,)}'$	time-averaged fluctuating quantity
$(\,)'',\tilde{(\,)}''$	Favre-averaged fluctuating quantity

1. INTRODUCTION

1.1 General Introduction

Jets and sprays are classical single and multiphase flows which have been extensively studied to improve understanding of fluid dynamics and transport. In contrast, gas jets in liquids have been studied very little. This is surprising and unfortunate. A gas jet in a liquid is the density inverse of a spray which provides a new perspective from which to study multiphase flows. Furthermore, gas injection in liquids is of importance in its own right for several applications, e.g., metal combustion for compact closed power production systems (SCEPS), direct-contact condensers, gas dissolution systems, reservoir destratification, nuclear reactor pressure suppression systems, etc. The present investigation considers aspects of gas injection into liquids, motivated by these applications.

Research issues concerning gas jets in liquids include: interaction of shock waves with liquid/gas interfaces, since gas jets in liquids generally operate with underexpanded jet exit conditions; the entrainment and mixing of the flow, which involves multiphase interactions in a turbulent environment, e.g., turbulent dispersion and turbulence modulation; the structure of the flow, since many applications require information concerning the extent and penetration of void volume; and the topography of the flow, which involves formation of drops and bubbles in various regions. Currently, no theoretical understanding exists to deal with any of these problems; therefore, existing successful designs have been achieved by expensive and time-consuming cut-and-try methods. This inhibits exploitation of innovative concepts like SCEPS.

In the following, past work on gas jets in liquids will be reviewed, prior to stating the specific objectives of the present study. The discussion begins with past work in this laboratory.

1.2 Penn State Studies

Several earlier studies of gas jets in liquids have been completed in this laboratory. The work includes noncondensing gas jets in liquids (Tross, 1976; Sun, 1985; and Sun and Faeth, 1985), condensing gas jets in liquids (Kerney et al., 1972; Weimer et al., 1973; and Chen and Faeth, 1982), and reacting gas jets in liquids (Avery and Faeth, 1975 and Chen and Faeth, 1983).

The earliest experimental studies were confined to gross parameters like the length of the vapor or gas-containing region and temperature profiles downstream of the multiphase flow region in condensing jets (Kerney et al., 1972; Weimer et al., 1973; and Avery and Faeth, 1975). Unchoked jets were found to be unstable due to liquid slugging into the injector passage; therefore, measurements were confined to underexpanded jets. Analysis was also undertaken, based on an integral model of turbulence and the locally homogeneous flow (LHF) approximation, which is widely used to analyze multiphase flows (Soo, 1976; and Wallis, 1969). The LHF approximation implies infinitely fast interphase transport rates and local instantaneous thermodynamic equilibrium, i.e., velocity differences (slip) between the phases are neglected and local phase and chemical equilibrium are assumed to be maintained. This analysis successfully correlated measurements of the length of the vapor-containing region. The fact that reacting and condensing vapor jets were handled with equal success justified analogy between these systems (Avery and Faeth, 1975). Treatment of external expansion was crude, however, and predictions of flow widths were inaccurate using the integral model.

Integral models do not provide a very satisfying picture of flow structure and have little potential for dealing with external expansion in a rational manner; therefore, the next stage of the work involved development of a higher-order turbulence model of the process (Chen and Faeth, 1982, 1983). This analysis generally followed the conserved-scalar approach of Bilger (1976) and Lockwood and Naguib (1975) which provided a successful treatment of constant density, variable density and combusting turbulent jets during other work in this laboratory (Jeng and Faeth, 1984; Shearer et al., 1979; Mao et al., 1980). The LHF approximation was used for this analysis while only nearly-adapted jet exit conditions were considered to avoid problems of external expansion.

A key feature of the use of the LHF approximation is that consideration of various systems only requires construction of state relationships between scalar properties (temperature, density, species concentrations, etc.) and the instantaneous mixture fraction (the fraction of mass at a point which originated from the injector). This computation is straightforward and only involves conventional adiabatic mixing or adiabatic reaction equilibrium calculations of fundamental thermodynamic theory. The turbulence model combined with the LHF approximation was successful in predicting the length of the vapor or gas containing region of both condensing and reacting jets, with all empirical parameters in the turbulence model fixed at values appropriate for constant-density single-phase jets (Chen and Faeth, 1982, 1983).

The most recent work in this laboratory has involved analysis and measurements for bubbly jets with nearly monodisperse bubbles sizes in the initial flow, e.g., noncondensing air into water (Sun, 1985; Sun and Faeth, 1985) and condensing carbon dioxide into water (Sun et al., 1985 a,b). The objective was to gain a better understanding of the limitations of LHF analysis and to begin development of more complete separated flow analyses of the process.

Measurements emphasized nonintrusive methods to provide reliable data for evaluation of analysis. This included phase velocities using laser Doppler anemometry; void volumes and bubble sizes using flash photography, and bubble number fluxes using Mie scattering from a laser light sheet. These techniques, however, are all limited to dilute concentrations of the dispersed (bubbly) phase.

The LHF analysis was evaluated using the new bubbly jet data. Two separated flow models were also developed which allow for finite interphase transport rates: (1) a deterministic separated flow (DSF) model which allows for slip between bubbles and liquid but ignores bubble/turbulence interactions; and (2) a stochastic separated flow (SSF) model which allows for both slip and bubble-turbulence interactions by random-walk computations of bubble motion.

A version of the SSF analysis also considered turbulence modulation, e.g., the effect of turbulence/bubble interactions on turbulence properties of the continuous phase (Al Taweel and Landau, 1977). The separated flow analyses employ the same turbulence model as the LHF analysis and were extensively evaluated during companion studies of particle-laden jets and sprays in this laboratory (Shuen et al., 1983a, 1983b, 1984; Solomon et al., 1984a, 1984b).

Comparison between predictions and measurements indicated that the LHF model performs reasonably well near the injector, where the maximum bubble slip velocities are small in comparison to mean flow velocities. The SSF model yielded reasonably good predictions throughout the flow. SSF analysis was particularly successful in correctly predicting the evolution of void fraction distributions from near-injector conditions, where bubbles approach

the LHF approximation, to conditions far from the injector, where turbulent dispersion of bubbles is slower than the dispersion of liquid due to effects of slip induced by buoyancy. In spite of its wide use in current models of sprays (Faeth, 1983), the DSF model performed poorly everywhere and appears to be of little value for treating gas injection into liquids. The results suggest continued potential for LHF analysis of high-velocity complex multiphase processes occuring near gas injectors, where the size distributions of dispersed phases (bubbles or drops) are normally not known. The SSF analysis provides a rational basis for evaluating effects of finite interphase transport rates far from the injector, based on estimates of the maximum likely sizes of dispersed phases.

1.3 Related Studies

Past structure measurements of condensing jets are very limited due to experimental difficulties for high void fraction multiphase flows. Earliest work by Cumo et al. (1978), Kudo et al. (1974), Lee et al. (1979), Stanford and Webster (1975) and Young et al. (1974) measured only gross features like the length of the vapor-containing region. Relevant portions of this data were used to evaluate the LHF analysis for condensing vapor jets (Chen and Faeth, 1982). Bakaklevskii and Chekhovich (1978) report temperature and dynamic pressure profiles in condensing plane jets in coflow, however, the measurement accuracy and flow conditions are too uncertain to provide more than a rough guide to flow structure.

In response to problems of designing pressure suppression systems for nuclear reactors, Chan (1974), Chun and Sonin (1984), Lambier and Chow (1984) and Simpson and Chan (1982) have measured static pressures near the injector exit during subsonic injection of condensibles into subcooled liquids. Pressure pulsations are very large at some conditions and have been correlated empirically. These pulsations appear to be related to mixing and collapse of large eddy structures in the flow, however, existing information is too limited to assess this effect.

Structure measurements for noncondensing gas injection into liquids are more numerous. Abdel-Aal et al. (1966) measured interfacial area by a nonintrusive technique, however, these measurements were confined to a region far from the point of injection. Goldschmidt et al. (1971) studied round jets containing nitrogen bubbles with probes, which are subject to large and poorly defined experimental uncertainties (Tross, 1976). More reliable results have been obtained using nonintrusive methods, e.g., laser Doppler anemometry for phase velocities and laser absorption for void fractions (Mahalingen et al., 1976; Ohba et al., 1977; and Ohba, 1979). Similar to structure measurements in this laboratory, however, these techniques are limited to low void fraction regions of the flow.

A particularly comprehensive study of bubbly flow with moderate void fractions (up to 44%) was conducted by Serizawa et al. (1975). This investigation involved the use of tracers and probes to measure void fraction, phase velocities and turbulent diffusivities of bubbly flow in a round pipe. Several other studies using similar techniques in pipes have also been reported, cf., Serizawa et al. (1975) for citations. However, in addition to uncertainties of probes, this flow configuration is dominated by wall effects and is not very satisfactory for evaluation of analysis for the free shear flow of submerged gas jets in liquids.

For flow stability, condensing gas jets in liquids normally are underexpanded. Past studies of gas jets in liquids have not considered the external expansion process, aside from peripheral observations by Kerney et al. (1972) for steam injection into subcooled water.

Adapted (exit and ambient pressures the same) single-phase gas jets have received far more attention. Measurements of mean and turbulent velocities, turbulent stresses, and mean and fluctuating concentrations have been completed for a wide variety of constant and variable density jets. Birch and Eggers (1973), Jeng and Faeth (1984) and Shearer et al. (1979) review recent work in the field.

Underexpanded gas jets and supersonic gas jets have been studied due to their relevance to base-pressure problems and exhaust plume signatures. Recent experimental work, including review of earlier literature, is presented by Addy (1981), Birch and Eggers (1973), Eggers (1966), Flack and Thompson (1977), Lau et al. (1979), and Lau (1980). Most of these measurements are limited to static pressure distributions along the axis of the flow. Addy (1981) uses shadowgraphs to determine the size and location of shock disks which appear downstream of the nozzle for high nozzle pressure ratios and also finds significant differences in the character of the flow field for different nozzle geometries (most of which had relatively small length-to-diameter ratios). More recent work by Lau and coworkers (1979, 1980), and Flack and Thompson (1977) have used laser Doppler anemometry to measure the velocity distribution in supersonic jets -- showing feasibility of this technique. Robinson et al. (1979) also employ nonintrusive techniques of infrared spectroscopy to obtain mean stagnation temperature ratios for supersonic jets.

Computations of underexpanded jet flows have also proved to be very challenging and are not well established due to uncertainties in numerics and lack of data on turbulence properties to assess turbulence modeling approximations. Vatsa et al. (1981, 1982) report calculations for slightly underexpanded jets using a quasiparabolic algorithm and an empirical algebraic turbulence model. Comparison between predicted and measured static pressure distributions was very encouraging. The region near the exit of an underexpanded nozzle requires full consideration of the viscous Navier-Stokes equations since streamwise and cross-stream pressure gradients are significant and shock waves can appear in the flow. Mikhail et al. (1980) report some computations along these lines for a nozzle boat-tail configuration.

More recently, Dash et al. (1985) and Seiner et al. (1985) report development of an analysis of turbulent underexpanded jets, using several contemporary turbulence models. Comparison between predictions and the data base discussed earlier was encouraging.

Computations conducted for SCRAMJET flow fields are also relevant to predictions of underexpanded jets. Berman et al. (1983), Drummond and Weidner (1982) and Sindir and Harsha (1984) report recent calculations of this type. Numerical methods following MacCormack (MacCormack and Lomax, 1979) were reasonably successful for algebraic turbulence models but convergence problems were encountered when higher-order turbulence models were used. These difficulties were attributed to the stiffness of the governing equations for turbulence quantities (Sindir and Harsha, 1984). A new unconditionally-stable algorithm has been proposed by MacCormack (1982) which might circumvent this difficulty, however, application to flowfields similar to the ones considered by Sindiar and Harsha (1984) has not been reported as yet.

Clearly, existing information on underexpanded single-phase gas jets is very limited and numerical methods for computing these flows are not highly developed. Comparable work for multiphase flows is virtually nonexistent.

1.4 Specific Objectives

The preceding discussion suggests that there is a good analogy between condensing vapor jets and more complex reacting gas jets in liquids. Existing information on condensing vapor jets, however, is not very complete and reliable methods for predicting the structure of these flows have not been demonstrated--aside from research in this laboratory at the limit of very low void fractions. Using existing measurements of gross quantities, the LHF model exhibits promise for predicting complex condensing jet structure in the region near the injector, however, structure measurements needed to fully assess predictions are not available. The SSF model shows potential for treating effects of finite interphase transport rates, based on existing measurements at low void fractions, but more information is needed concerning near-injector processes in order to provide initial conditions and bubble size distributions required to initiate these calculations. Effects of external expansion, which are important for practical condensing jets, are poorly understood for single-phase flows and have not been studied for multiphase flows.

The present investigation initiates study of these problems. Over the course of the work, it is planned to systematically consider the following flows:

1. Water jets in water (a single-phase, constant density baseline).
2. Air jets in air (a single-phase compressible baseline).
3. Air jets in water (a compressible noncondensing multiphase flow).
4. Carbon dioxide jets in water (a compressible condensing multiphase flow).

In contrast to most past work of multiphase jets, the present investigation will emphasize high void fraction compressible flow processes near the jet exit.

The purpose of the present, short-duration, study was to develop test apparatus and instrumentation for the investigation.

Two test arrangements were considered, as follows: (1) an underexpanded air jet in air, and (2) water and air jets in water. The resulting test arrangements, plans for analysis of the flows, and some initial experimental results are discussed in the following.

2. AIR-JET-IN-AIR STUDY

2.1 Introduction

Work on air jets in air involved development of the test apparatus and a portion of the instrumentation. Work was also undertaken to initiate analysis for subsonic jet conditions, which only involves minor changes from past methods. Finally, experiments were begun with the apparatus, considering flow visualization by continuous and flash Schlieren photography. These activities are discussed in more detail in the following.

2.2 Experimental Methods

2.2.1 Test Apparatus

The overall test arrangement for the air jet apparatus is illustrated in Fig. 1. The test arrangement itself is relatively simple, involving an air supply and a long length-to-diameter passage to provide a round jet with various degrees of underexpansion. Major measurements involve laser Doppler anemometry (LDA), for velocities; Rayleigh scattering (RS), for density; and laser-induced fluorescence (LIF) for mixing levels (or concentrations). The optical arrangements for these three systems are sketched in Fig. 1; they will be discussed in more detail in the next section.

The test apparatus is located in the Gas Dynamics Laboratories of the University of Michigan. The air supply is provided by laboratory facilities, consisting of dried and filtered air drawn from a storage vessel (storage pressures in excess of 10MPa, dew point less than 240K). Air flow rates are controlled with pressure regulators and metered with critical flow orifices, which are calibrated with positive-displacement meters. The temperature of the inlet air is monitored with thermocouples. Seeding materials in the flow include oil particles, for LDA measurements; and iodine vapor, for LIF measurements. Since these materials are objectionable in the test area, the jet flow is exhausted through a vent to the outside.

Optical components are mounted rigidly; therefore the nozzle is traversed to measure flow properties at various points. A sketch of the nozzle and traversing system appears in Fig. 2. Air is supplied to the nozzle through a flexible hose. The inlet of the nozzle is fitted with a flow straightener followed by a circular-profile contraction (7:1 area ratio) to the nozzle passage. The nozzle passage has a constant diameter, 9.5 mm, and a length of 50 passage diameters. Pressure is monitored at the inlet of the contraction, and at four locations near the exit -- the latter to provide the exit-plane pressure by extrapolation.

The nozzle is mounted on two pairs of linear bearings to provide traversing in the horizontal plane. The traverses are controlled by a computer (IBM system 9000) using two motor-driven Unislide assemblies. The mounting stand itself has four screw adjustments to control the height and angle of the flow.

Operation of this arrangement is very noisy, particularly for high levels of underexpansion. Therefore, the system is operated remotely from a room adjacent to the test cell.

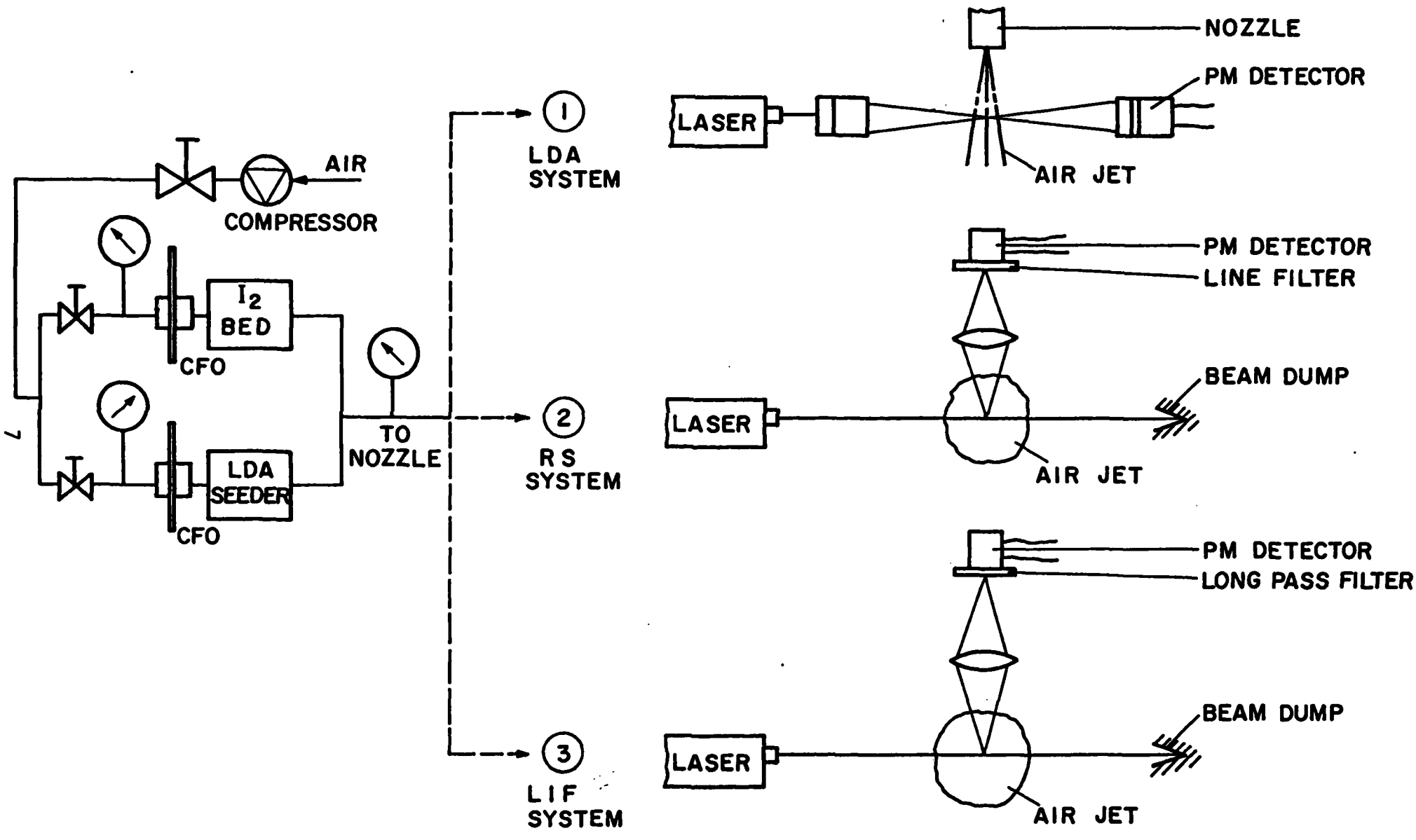

Figure 1. Sketch of the airjet apparatus.

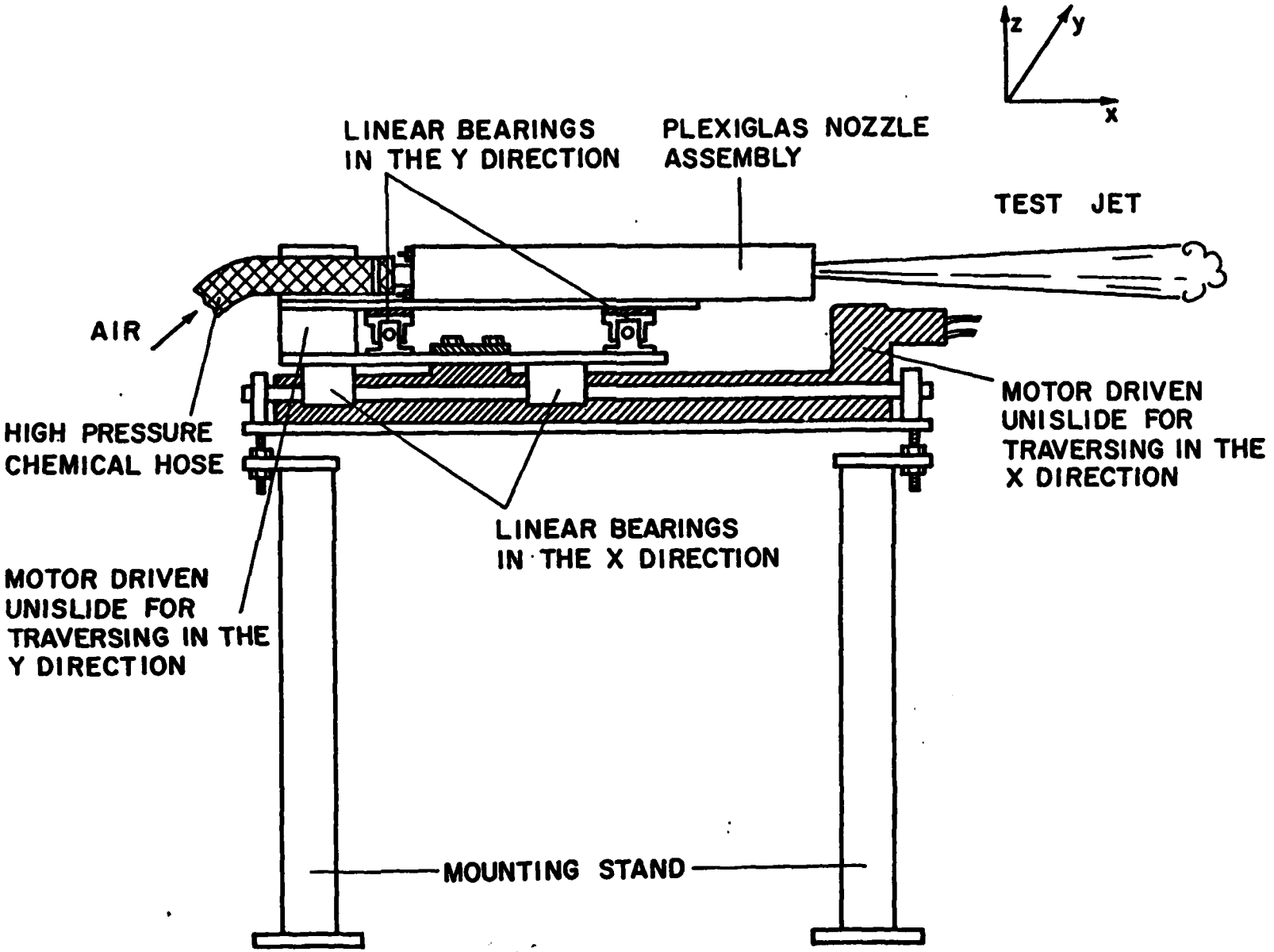

Figure 2. Sketch of the nozzle and traversing system.

2.2.2 Instrumentation

Laser Doppler Animometry (LDA). The LDA arrangement is illustrated in Figs. 1 and 3. The system shown has the detector in the forward scattering direction. Actually detection at right angles, from the bottom looking upward, is used for current tests, in order to provide better spatial resolution. A 4W argon-ion laser (Coherent, INNOVA 90-4 with Model 923 Etelon Assembly) is used in the single-line (514.5 nm) mode.

A single-channel LDA arrangement is used, with a Bragg cell frequency shifter to avoid problems of directional ambiguity and flow reversals near the edge of the flow. The optical arrangement yields a fringe spacing of 14.0 μm and a measuring volume having a diameter and length of 260 μm. The relatively-large fringe spacing is used to control signal frequencies in high-velocity regions of the flow. The relatively-small measuring volume dimensions reduces effects of gradient broadening (estimated) to less than 1%.

The LDA actually measures the velocity of small seeding particles in the flow, which must be small enough to accurately follow the gas. DOP particles, 100-300 nm in diameter, are used for present work. The particles are generated in a nebulizer system which receives a portion of the inlet flow. These particles are adequate to follow mean velocities but will attenuate signals from the highest frequences in the flow and broaden signals downstream of shock waves for roughly 1 mm. Subsequent work will consider development of a more satisfactory seeding arrangement.

Seeding densities provide less than 0.3 particles/measuring volume, while seeding levels are high in comparison to flow length scales; therefore, a low burst density and high data density LDA signal is obtained. This allows reduction of data as time averages by averaging the analog output of the burst counter signal processor (TSI Model 1990C), without problems of velocity bias. The output signal is acquired using a 12 bit LeCroy Model 8212A/8 A/D converter and Model 8800A 32K memory, and an IBM system 9000 computer. This arrangement allows block acquisition of 32000 samples while the 52Mb storage capacity of the computer allows acquisition of blocks of data well beyond requirements of the present study. While a single-channel arrangement is used, all components of velocity and second-order velocity correlations can be obtained by rotating the optical plane of the instrument, similar to past work (Schuen et al., 1984).

Rayleigh Scattering (RS) System. Sketches of the RS system appear in Figs. 1 and 4. The technique involves measuring laser light which is elastically scattered from molecules. The intensity of the scattered light can be related to the number of molecules within the control volume, and thus the density. System response is very rapid; therefore, density fluctuations can be resolved even in high-speed flows.

The present system is based on the same argon-ion laser as the LDA system. The 488 nm (blue) line of the laser is used for RS measurements since this yields the strongest scattering signal. The scattered signal is observed at right-angles to the laser beam, but in the same plane. This provides reasonably good spatial resolution, 500 μm diameter measuring volume, with polarization vectors aligned to give maximum signal-to-noise ratio. A laser-line filter in front of the detector minimizes background effects. A portion of the laser beam is split from the main beam and its intensity is measured with a second detector, to monitor beam power. The data acquisition system is similar to the LDA system.

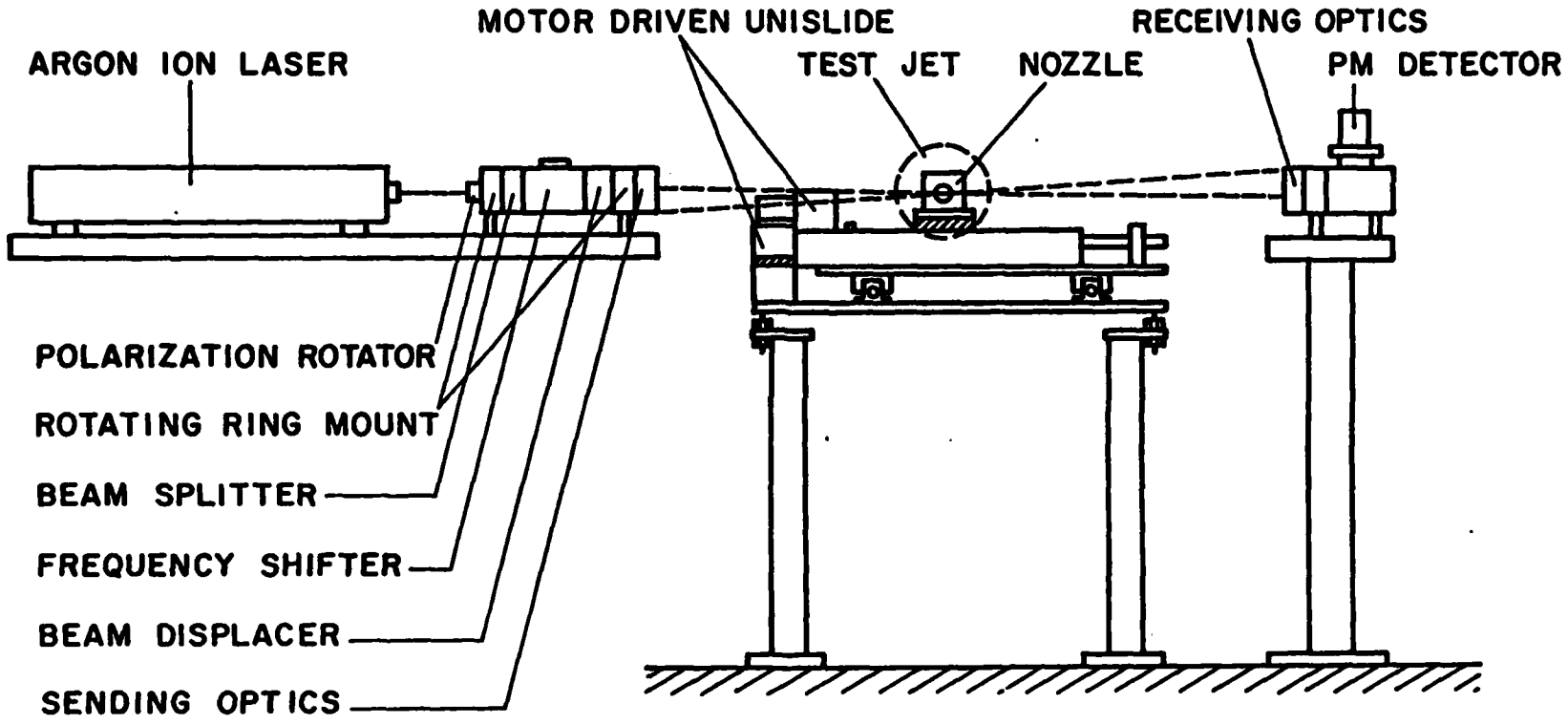

Figure 3. Sketch of the LDA system.

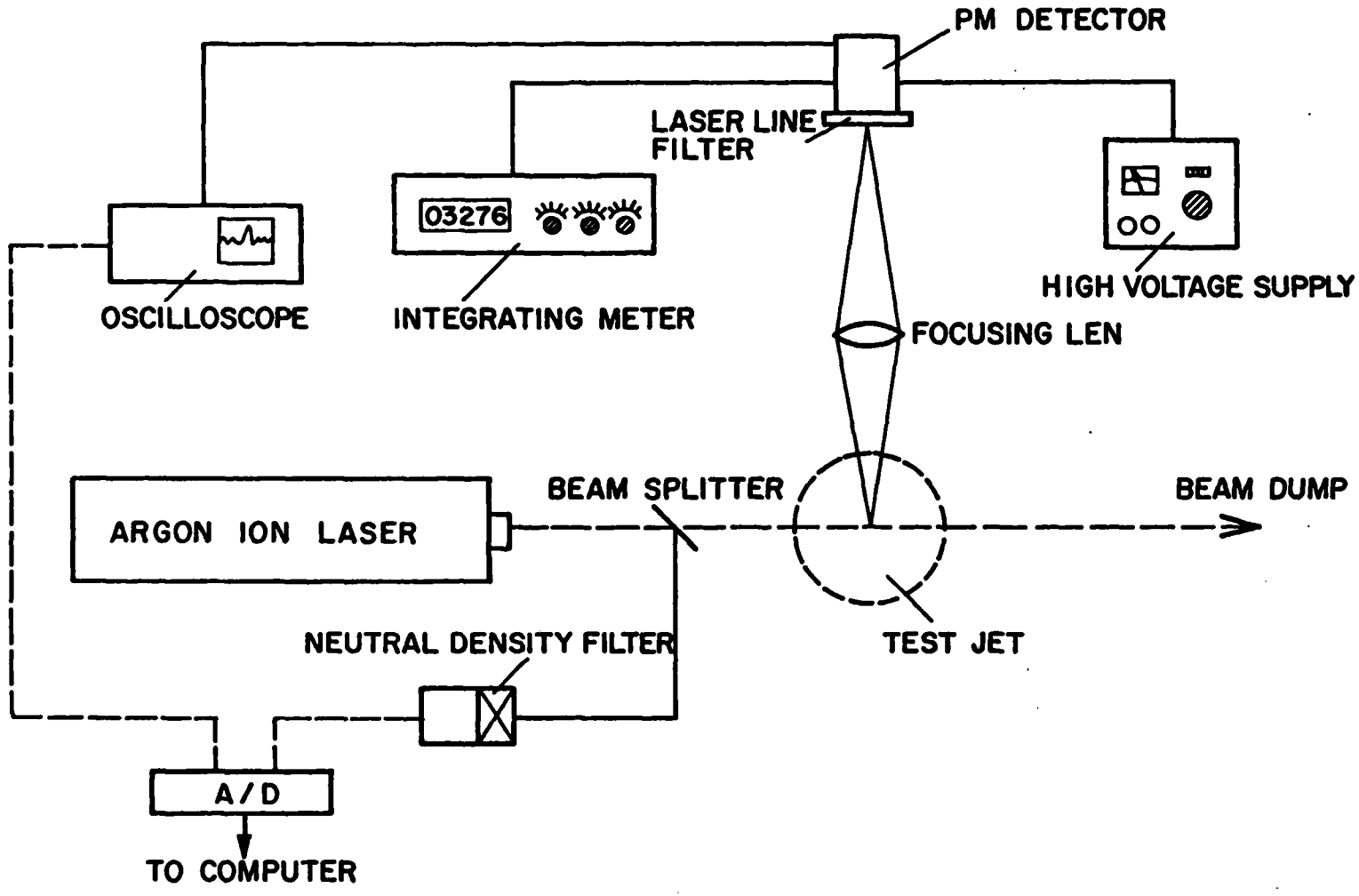

Figure 4. Sketch of the Rayleigh scattering system.

Laser-Induced Fluorescence (LIF) System. Sketches of the LIF system appear in Figs. 1 and 5. The signal originates from inelastic scattering of light from the laser beam, due to the presence of iodine tracer in the jet flow. The intensity of this signal is proportional to the concentration of iodine molecules in the measuring volume; therefore, the measurement provides the extent of mixing of the flow with the surroundings.

The present system is based on an arrangement developed by Lai et al. (1985) in this laboratory. The argon-ion laser used for LDA and RS measurements is also used for this system, but operating at the 514.5nm line. Laser power is monitored similar to the RS system. In addition, a third beam is split from the main beam and directed across the exit of the jet. The transmitted power of this beam is measured, giving the concentration of iodine seeding gas at the exit by the degree of absorption. The two monitoring systems provide a means for correcting the LIF signal for both beam power and seeding level fluctuations.

The LIF signal is observed from a position perpendicular to the laser beam, to improve spatial resolution. The measuring volume size is controlled by the laser beam diameter and a field stop in the detector optics. The present configuration yields a cylindrical measuring volume having a diameter of 1 mm and length of 1.3 mm.

The signal scattered to the detector includes a relatively strong Raleigh scattered signal along with the LIF signal. A typical spectrum is illustrated in Fig. 6. A low-resolution monochrometer (8nm band-width) was used for these measurements; therefore, the laser line appears as a strong band and many details of the spectrum are lost. However, the LIF signal at longer wavelengths than the laser line is clearly evident. The laser line must be blocked to obtain a signal proportional to the iodine concentration. This is done by installing a series of long pass filters in front of the detector. The resulting spectrum after filtering is also shown in Fig. 6. The technique clearly eliminates signal from the laser line. Calibration shows that the remaining filtered signal is a linear function of the concentration of iodine.

Reabsorption of fluorescence and absorption of the laser beam itself, by iodine, must also be considered. However, both effects are small for present test conditions, since beam lengths through the iodine-containing portions of the flow are relatively short.

The air flow is seeded with iodine by passing a portion through a bed of iodine crystals. The bed operates at room temperature and the flow is saturated at the exit of the bed; therefore, the concentration of iodine vapor, which is proportional to the iodine vapor pressure, varies with changes in room temperature. These changes, however, are considered by the monitoring system described earlier. The iodine crystals are reagent grade, having a flake shape (initially 2-8mm in diameter and 0.5mm thick). Iodine vapor, even at low concentrations, is relatively corrosive; therefore, all components downstream of the iodine seeder are plexiglass, plastic or brass, which have reasonably good corrosion resistance.

Signals from the three detectors in the LIF system are sampled and processed with a computer, similar to the LDA measurements.

Flow Visualization. Three techniques are used for flow visualization, as follows: continuous Schlieren, spark Schlieren and light-sheet photography. The Schlieren systems are based on 150mm diameter parabolic reflectors having focal lengths of 1220mm. The continuous light source is provided by a 100W mercury arc. The spark light source is provided by a 10J discharge for a duration of 100ns.

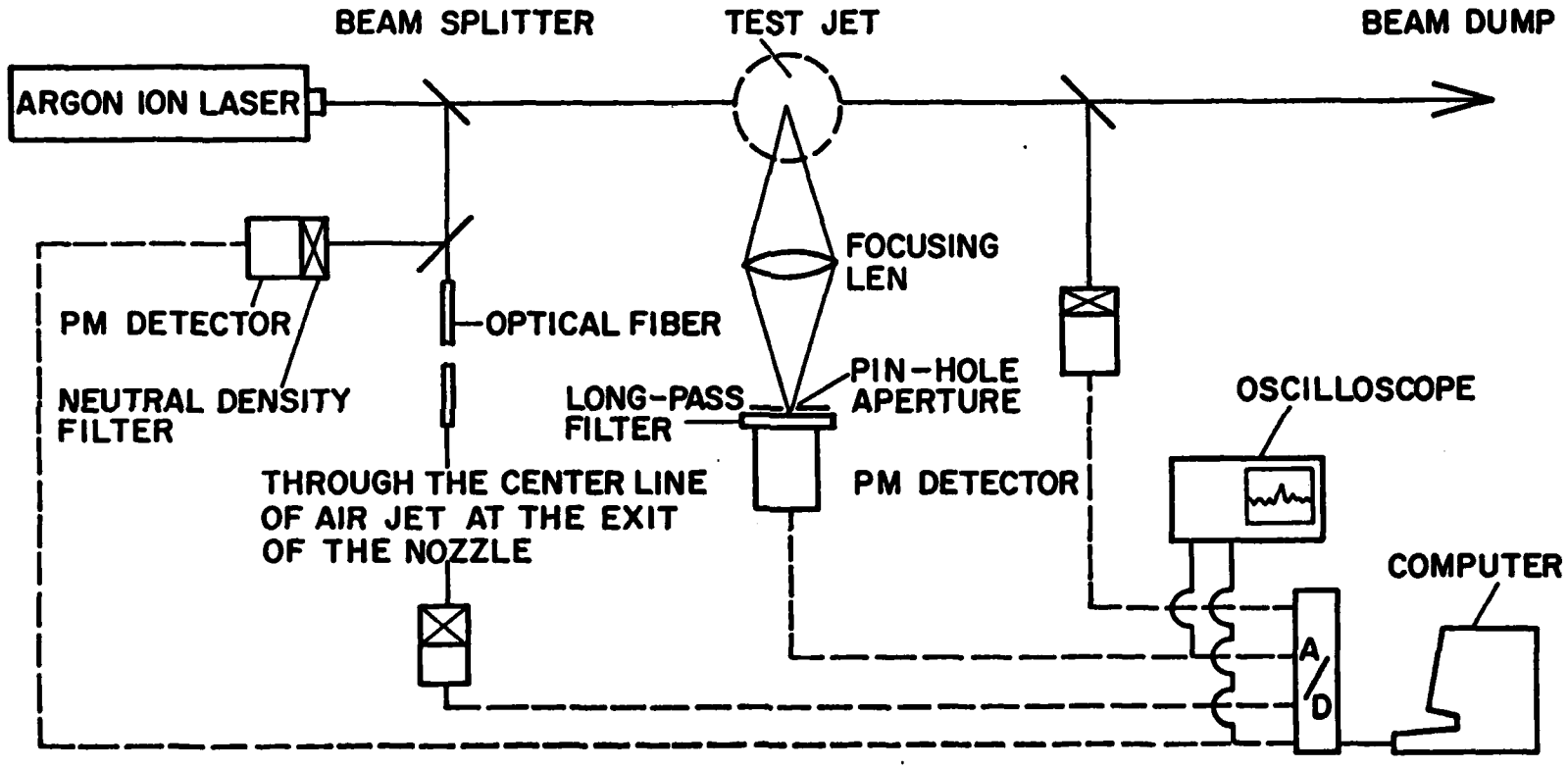

Figure 5. Sketch of the laser-induced fluorescence system.

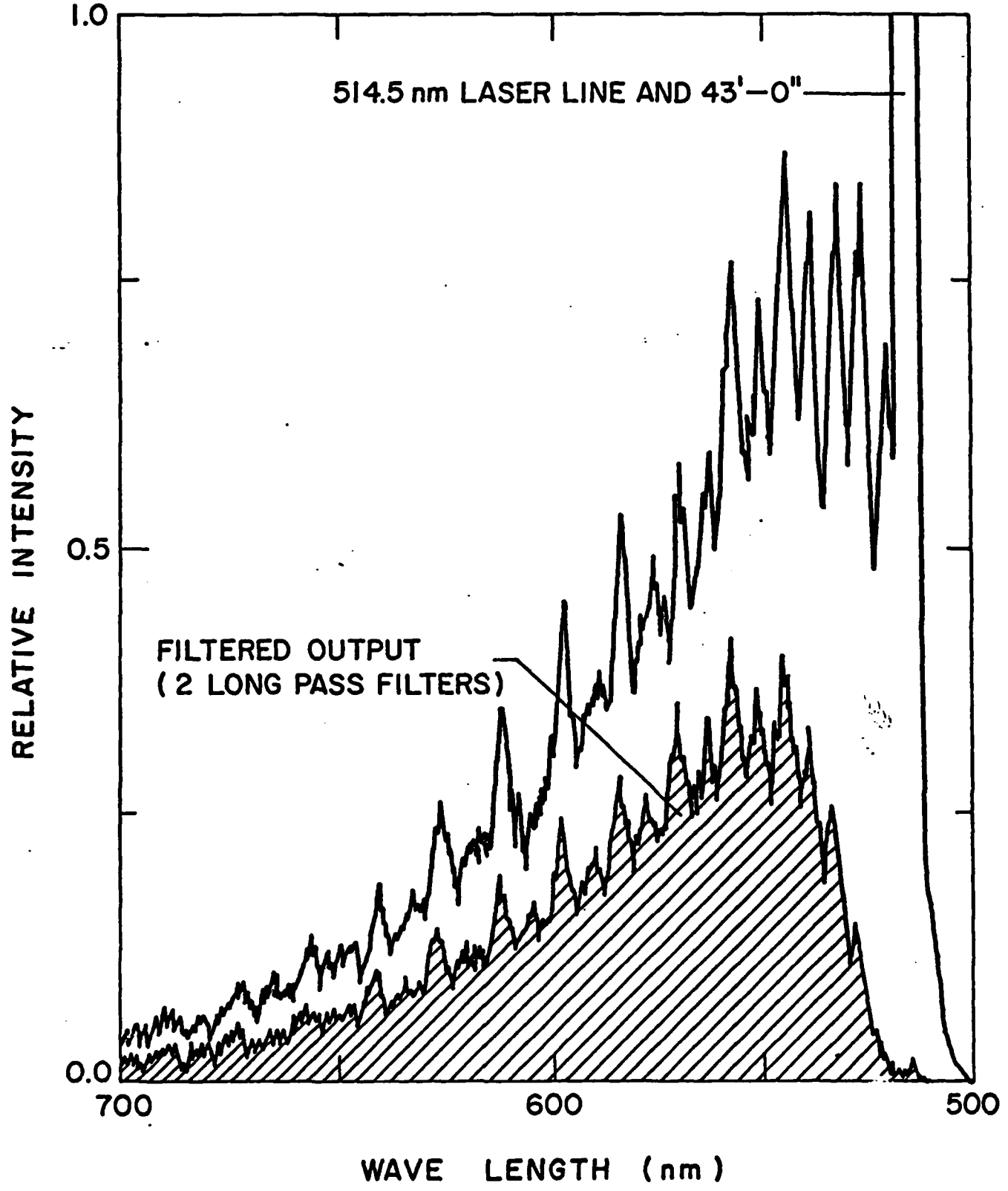

Figure 6. Original and filtered LIF spectrum.

The light sheet photography is based on Mie scattered light from seeding particles in the flow as they pass through a light sheet. The light sheet is generated by a Xenon Corp. Model 457, Pulser Flashlamp system yielding 10J per pulse with a flash duration of ca. 1μs. A system of lenses, spherical and cylindrical, spreads the light into a sheet which can be directed parallel or normal to the axis of the jet.

The jet flow is seeded with particles using the nebulizer, similar to the LDA system. However, the surroundings are particle-free. Therefore, light scattered from the particles provides an indication of the extent and deformation of the jet flow. The seeding particles are too large (100-300nm) to diffuse at the molecular level, unlike gas molecules, but this is not very significant at the high Reynolds numbers of presents flows. A more significant effect is the finite length of the flash duration, which will allow particles to move as much as 500μm in the highest-speed regions of the flow. This tends to wash out the fine details of the flow.

2.3 Theoretical Methods

Theoretical considerations thus far have been limited to adapted (exit plane and ambient pressure equal) sonic and subsonic flow. Analysis at this limit follows past practice, c.f., Shuen et al (1983b) or Sun and Faeth (1985).

Analysis is limited to steady (in the mean) single-phase round turbulent jets having negligible effects of buoyancy. The conserved-scalar formalism is used to find scalar properties (Bilger, 1976; Lockwood and Naguib, 1975). This is not a necessary part of the analysis of subsonic single-phase jets, but is required for consistancy with LHF analysis. Turbulence properties are found using a k-ε-g model, which has been shown to give good predictions of mean and turbulent properties of single-phase jets and related flows (Jeng and Faeth, 1984; Mao et al., 1980; Shearer et al., 1979; Shearer et al., 1983a, 1983b, 1984; Solomon et al., 1984a, 1984b; Sun, 1985; and Sun and Faeth, 1985). Major assumptions are: exchange coefficients of all species and heat are the same, buoyancy only affects the mean flow, and mean kinetic energy, viscous dissipation and radiation are negligible. The assumption of equal exchange coefficients is widely recognized as being acceptable for high Reynolds number flows typical of gas injection systems (Faeth, 1983). Effects of buoyancy are small for present flows; therefore, considering effects of buoyancy on mean properties is sufficient to monitor any perturbation of the flow by this phenomenon. Neglecting mean kinetic energy, etc., is adequate for the relatively slow subsonic jets where baseline tests will be undertaken, however, this assumption will have to be relaxed for analysis of the bulk of the data.

Analysis is limited to boundary-layer flows with no zones of recirculation, which is typical of subsonic gas jets in liquids. The test flows were axisymmetric with no swirl; therefore, the analysis is posed accordingly. This approach assures adequate numerical closure with modest computational costs and also corresponds to cases where turbulence models were developed and have high reliability.

The analysis is formulated in terms of Favre- or mass-averaged properties rather than Reynolds- or time-averaged properties. This simplifies treatment of variable-density flows since ad hoc neglect of terms involving density fluctuations is avoided. A single set of empirical constants has been found which satisfactorily predicts both constant- and variable-density flows (Jeng and Faeth, 1984). These constants are virtually identical to the earliest versions of this type of analysis (Lockwood and Naguib, 1975).

The Favre-averaged governing equations are:

$$\frac{\partial}{\partial x}(\bar{\rho}\tilde{u}\tilde{\phi}) + \frac{1}{r}\frac{\partial}{\partial r}(r\bar{\rho}\tilde{v}\tilde{\phi}) = \frac{1}{r}\frac{\partial}{\partial r}(r\mu_{eff}\frac{\partial\tilde{\phi}}{\partial r}) + S_{\phi} \qquad (1)$$

where

$$\tilde{\phi} = \overline{\rho\phi}/\bar{\rho} \qquad (2)$$

is a Favre-averaged property while ϕ is a generic quantity. The source terms appearing in Eq. (1) are summarized in Table 1 along with the appropriate empirical constants. The turbulent viscosity is calculated from k and e in the usual manner.

$$\mu_t = C_{\mu}\bar{\rho}k^2/\varepsilon \qquad (3)$$

The boundary conditions on these equations are: u, f, k, ε and g are all zero at the edge of the flow, and gradients of these quantities are zero at the axis.

Initial conditions require profiles of u, f, k, and ε and g at the jet exit along with prescription of the exit plane pressure. By definition, $f = 1$ and $g = 0$. The remaining properties will be measured for present experiments. The variables u and k can be obtained directly from LDA measurements. The variable ε can be found by measuring the streamwise gradient of k at the exit.

The equations are solved using a modified version of the GENMIX algorithm (Spalding, 1977). Cross-stream grid nodes in the range 33-99 and streamwise step sizes chosen to be limited by 6% of the current flow width or an entrainment increase of less than 5% are used to obtain adequate numerical closure (flows with large density variations require more nodes).

With equal exchange coefficients and small kinetic energy effects and radiative heat losses, all instantaneous scalar properties (temperature, phase fractions, species concentrations, etc.) are only a function of the mixture fraction. This implies that instantaneous scalar properties can be found by simple adiabatic mixing (or chemical equilibrium) calculations where f kg of injector fluid and (1-f) kg of ambient fluid are adiabatically mixed and brought to thermodynamic equilibrium. This is a straightforward calculation for any flow configuration, but does allow for substantial complications due to effects of dissociation or the appearance of a variety of phases. The relationships between scalar properties and f are termed state relationships. Several examples of state relationships and their construction appear in the literature (Bilger, 1976; Chen and Faeth, 1982,1983; Faeth, 1983; and Jeng and Faeth, 1984).

Solution of the governing equations provides a means of finding the Favre-averaged probability density function (PDF) of mixture fraction, $\tilde{P}(f)$, as described later. Given $\tilde{P}(f)$, the Favre-averaged mean value of any scalar property becomes

$$\tilde{\phi} = \int_0^1 \phi(f)\tilde{P}(f)df \qquad (4)$$

Table 1. Summary of source terms.

ϕ	S_ϕ
1	0
$\bar{u}$	$a\,(\rho_\infty - \bar{\rho})$
$\bar{f}$	0
k	$\mu_t \left(\frac{\partial \bar{u}}{\partial r}\right)^2 - \bar{\rho}\varepsilon$
ε	$C_{\varepsilon_1} \mu_t \frac{\varepsilon}{k} \left(\frac{\partial \bar{u}}{\partial r}\right)^2 - C_{\varepsilon_2} \bar{\rho} \frac{\varepsilon^2}{k}$
g	$C_{g_1} \mu_t \left(\frac{\partial \bar{f}}{\partial r}\right)^2 - C_{g_2} \bar{\rho} \frac{\varepsilon g}{k}$

C_μ	$C_{\varepsilon 1}$	$C_{\varepsilon 2} = C_{g2}$	C_{g1}	σ_k	σ_ε	$\sigma_f = \sigma_g$
0.09	1.44	1.87	2.8	1.0	1.3	0.7

where $\phi(f)$ is the state relationship for the property (Bilger, 1976). Similarly, time-averaged properties are found from

$$\tilde{\phi} = \bar{\rho} \int_0^1 (\phi(f)/\rho(f)) \tilde{P}(f) df \qquad (5)$$

where ρ, which is needed to solve the governing equations, is found by setting $\phi = 1$ in Eq. (5). Fluctuating scalar properties may also be found in a similar manner, e.g.,

$$\tilde{\phi}''^2 = \overline{\rho\phi}''^2/\bar{\rho} = \int_0^1 (\phi(f) - \tilde{\phi})^2 \tilde{P}(f) df \qquad (6)$$

and

$$\bar{\phi}'^2 = \int_0^1 ((\phi(f) - \tilde{\phi}(f))^2/\rho(f)) \tilde{P}(f) df \qquad (7)$$

To complete the formulation, a functional form must be assumed for $\tilde{P}(f)$, although the specific form does not have a strong effect on predictions of mean properties. A clipped Gaussian function has been used in work to date. This is a two-parameter distribution whose specification is completed by finding its most probable value and variance. These quantities can be found from the moments of the distribution by noting

$$\tilde{f} = \int_0^1 f \tilde{P}(f) df \qquad (8)$$

$$g = \int_0^1 (f - \tilde{f})^2 \tilde{P}(f) df \qquad (9)$$

Since $\tilde{f}$ and g are known from solution of the governing equations, Eqs. (8) and (9) provide two implicit equations to find the parameters of the PDF. Solution of these equations is facilitated by a table constructed by Shearer et al. (1979).

This analysis can be applied to subsonic single and multiphase flows as it stands (the latter by use of the LHF approximation and both after definition of state relationships, Faeth (1983)). For subsonic air jets in air, density is nearly constant and the state relationships are linear functions of mixture fraction; therefore, the difference between Favre and Reynolds averages is negligible and mean scalar properties can be found immediately from properties at f, without recourse to integrating the PDF. This version involves no extension of past work and has been implemented on the University of Michigan computer system for evaluation of current experiments.

Calculations of major interest during the current investigation will involve patches of supersonic flow; therefore, the present analysis must be extended. This work will be undertaken during the next phase of the study.

2.4 Results and Discussion

During this report period, the test apparatus was designed, fabricated and finally assembled at the Gas Dynamics Laboratories of the University of Michigan. Initial tests were also completed, involving flow visualization to check operation of the system and obtain initial measurements of the shock structure of underexpanded jets. Findings thus far are preliminary, however, a portion of the results will be considered to indicate their nature.

A typical continuous Schlieren photograph of the air/air jet at an underexpanded condition is illustrated in Fig. 7. In this case, the exit plane pressure is 4.2 times higher than the ambient pressure. Major features of the flow are indicated in the sketch of the process illustrated in Fig. 8. An expansion fan at the exit of the passage initiates the pressure adjustment, but also creates a supersonic flow. The expansion waves are reflected from the edge of the flow (not shown) as compression waves, which steepen to form an oblique barrel shock wave. The barrel shock is propagated toward the centerline, but for the conditions shown it cannot reach this point and still properly accomplish turning of the flow. Instead it reaches a triple point at the intersection of a normal shock which crosses the centerline (Mach disk) and a reflected oblique shock. The reflected shock reaches the edge of the flow where it is reflected as an expansion fan to repeat the process again (modified by viscous effects). Viscous effects are important near the edge of the flow and in a mixing layer eminating from the triple point for this first shock cell. Subsequent cells have important effects of mixing over the entire flow, which tends to wash out the wave pattern. Most of the features shown in Fig. 8 can be found on the Schlieren photographs of Fig. 7.

Regions where viscous and mixing effects are important can be readily seen in spark Schlieren photographs. A typical example, for conditions similar to those used in Fig. 7, is illustrated in Fig. 9. The shock waves can still be seen as fine lines passing through the flow at the positions shown in Figs. 7 and 8. Dappled regions on this photograph give an indication of the growth of the jet mixing layer - which is very rapid near the end of the passage. The Mach disk mixing layer, however, is obscured since it is inside the jet mixing layer for the present axisysimmetric flow.

Similar measurements were made at several exit plane pressure levels to define major wave features of the flow. This includes the appearance, diameter and standoff distance of the Mach disk. Similar measurements have been reported by Addy (1981) for several nozzle conditions, but not including a long passage as in present tests, e.g., he used small length-to-diameter ratio contractions of various geometries. Preliminary results indicate qualitative agreement between the present findings and those of Addy (1981). However, differences are seen which can be attributed to the more fully-developed flow from the present passage, e.g., Mach disk diameters are somewhat smaller. These results will be reported subsequently.

2.5 Summary

The air/air jet apparatus has been assembled and initial flow visualization tests have been completed. The apparatus appears to be satisfactory for planned testing. The next phase of experimental work will involve flow visualization using light sheet photography and point measurements using the LDA, RS and LIF systems.

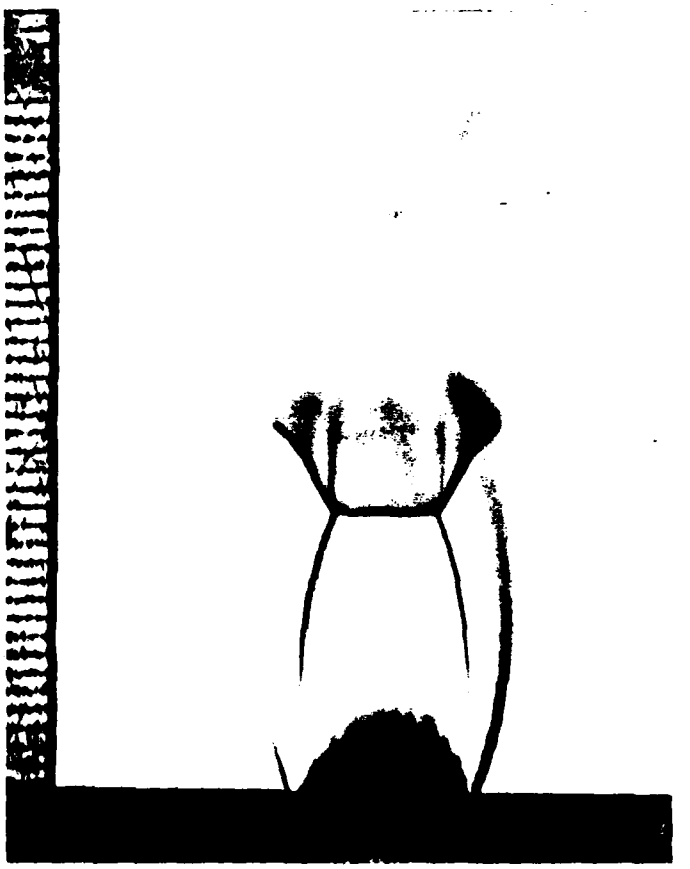

Figure 7. Typical continuous Schlieren photograph of an underexpanded sonic jet.

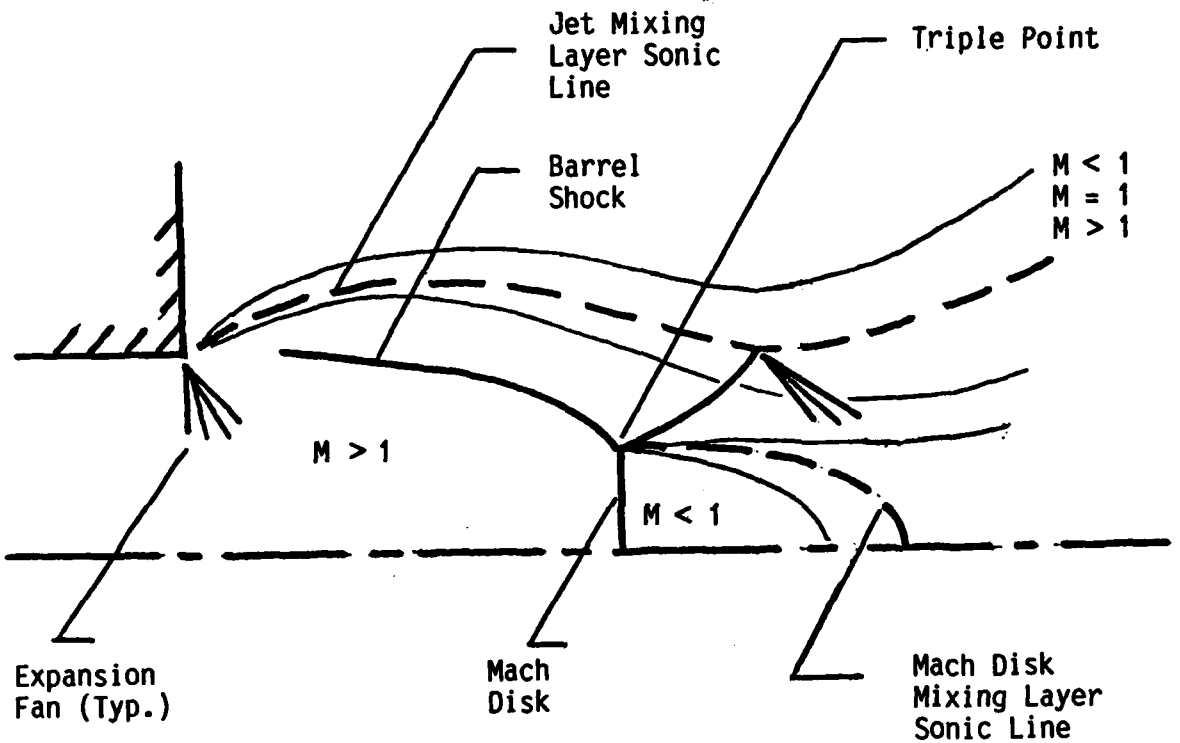

Figure 8. Schematic of near-field region of an underexpanded turbulent jet. Adapted from Dash et al. (1985).

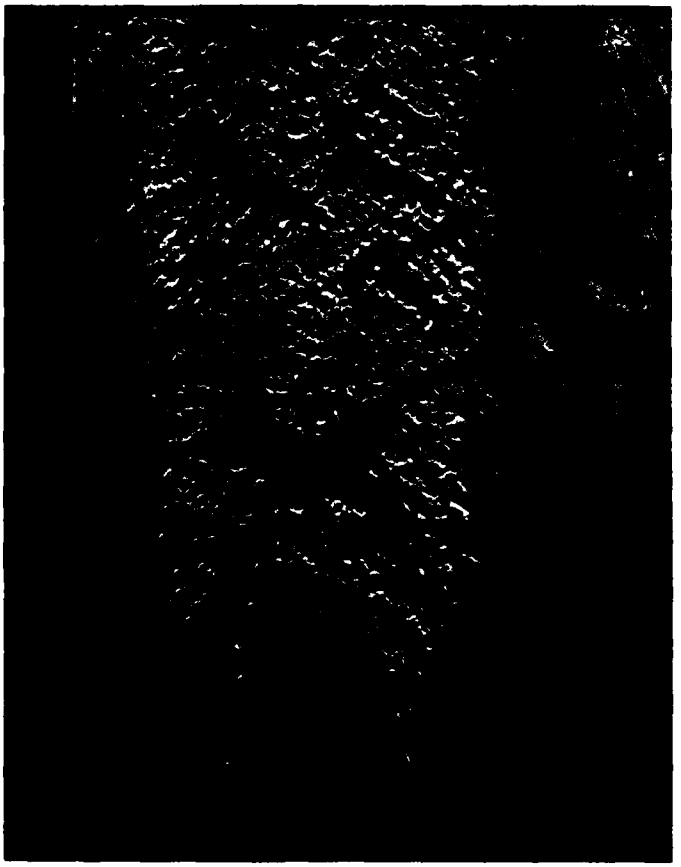

Figure 9. Typical spark Schlieren photograph of an underexpanded sonic jet.

Analysis of subsonic jet exit conditions has been implemented for evaluation with data from baseline tests. Extension to allow treatment of underexpanded jets will be undertaken during the next report period.

3. GAS-JET-IN-WATER STUDY

3.1 Introduction

The test apparatus for the gas-jet-in-water study was developed. Analysis for baseline tests of water jets in water, as well as for LHF analysis of subsonic air-jets-in-water, only required minor modification of the air jet analysis discussed in the previous section and was implemented as well. Finally, initial tests associated with apparatus design were undertaken in an apparatus developed during earlier work on multiphase flow. These activities are described more fully in the following.

3.2 Experimental Methods

3.2.1 Test Apparatus

The arrangement of the test apparatus is sketched in Fig. 10. The apparatus consists of a large water-filled tank, a traversable injector assembly, and instrumentation for nonintrusive velocity (LDA) and void fraction (gamma-ray absorption) measurements.

Measurements are obtained within a large rectangular (1m x 2m x 2m deep) tank. The tank is open at the top and has windows covering the full height of the four sides. This provides a reasonable simulation of a stagnant bath as well as flexibility in providing optical access for flow visualization and optical diagnostics.

The injector is mounted on a traversing system, looking vertically upward. The traversing system provides large traverses vertically and in one horizontal direction (along the 2m long sides) and a trim adjustment in the third direction (along the 1m side). This provides for profiles of flow properties along the jet axis and in one radial direction), with the trim adjustment used to set the measuring plane along the axis. The traversing gear itself is located outside the tank, with the injector mounted to a support rod which is kept out of the jet flow region.

Initial tests, to be described later, indicated that the injector exit should be screened to avoid problems of liquid slugging into the passage. Furthermore, the length of the injector assembly must be limited to provide an adequate region for measurements. Therefore, the injector design involves a plenum section, containing a honeycomb flow straightener, followed by a contraction to a short (L/d=1) constant-diameter passage (9.5 mm diameter) containing three course-mesh screens. The bottom of the injector is fitted with a purge line to remove water for tests involving air flow. The downstream end of the passage is centered in a flat block, which also helps to reduce effects of liquid slugging at subsonic conditions. In effect, the design is similar to the air jet system, except for the short passage and the use of screens.

The tank is fitted with an overflow line as well as a water fill line (the latter being just a hose). Water (for water jet tests) is provided by the local supply, metered with a valve, and measured with a rotameter. The air supply to the injector is provided in the same manner as the air jet tests; consisting of a pressure regular for flow control and a critical flow orifice for metering.

Preliminary tests showed that problems of liquid slugging into the injector passage are increased by the release of large bubbles or clumps of bubbles at the liquid surface. This disturbs the surface and causes pressure pulsations at the injector exit. This problem was

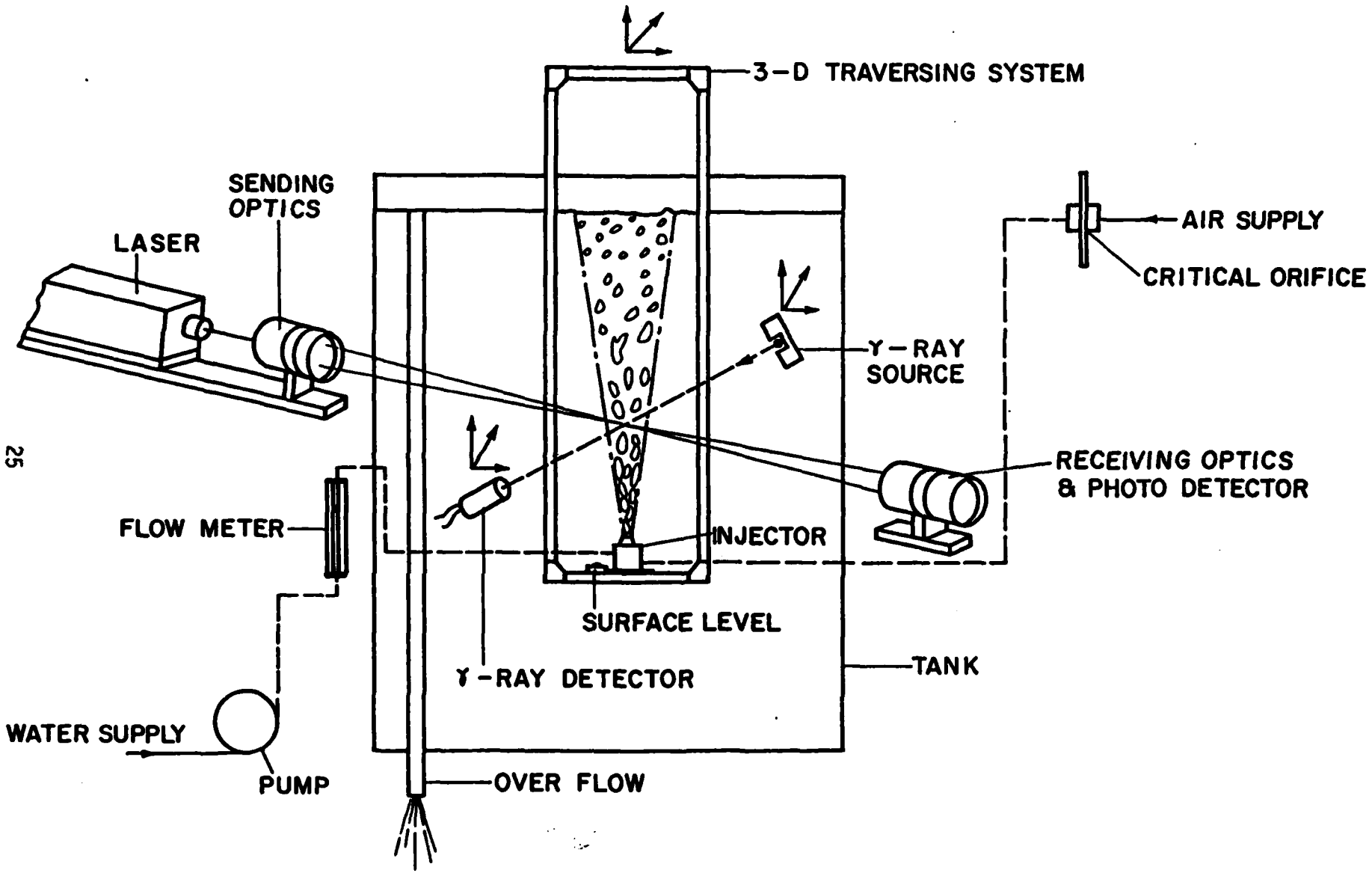

Figure 10. Sketch of the gas jet in water apparatus.

reduced by installing a deflector plate (not shown in Fig. 10) near the surface, which forces the bubbles to release from its periphery in a more stable and uniform manner (analagous to water spilling over the edge of a pool at the base of a fountain).

3.2.2 Instrumentation

Flow Visualization. Flash photographs are obtained for the near-injector region. The light source is a Xenon Corp. Model 457, Pulsar Flashlamp system yielding 10J per pulse with a flash duration of ca. 1μs. Photographs are obtained with an open camera shutter in a darkened room; therefore, the time of exposure is controlled by the duration of the flash, which is short enough to stop the motion for present test conditions. Direct visualization provides the most information for gas injection into liquids. This involves locating the camera near the flash lamp, with both viewing the flow.

Motion pictures are also planned, but have not been undertaken as yet. They will be obtained using high speed photography obtained with a Redlakes HyCam Camera (up to 10,000 pictures per second) available in this laboratory. These photographs will be obtained using scattered light from steady arc lamp sources--also available in this laboratory. The photographs will be analyzed to insure that liquid is not slugging into the injector. The boundaries of the multiphase flow region will also be measured, using image-processing equipment available at the University. These photographs will be taken so that the entire flow region can be observed. This provides direct information on phase intermittency which is useful for evaluating the analysis. The camera record can be arranged to show static pressure variations in the bath directly on the films. Therefore, effects of void collapse can be associated with the pressure traces--which is valuable for condensing jets where pressure fluctuations are important.

Laser Doppler Anemometry. LDA measurements of liquid velocities will be obtained for all liquid regions of the flow. This involves the entire flow field for the baseline water jet tests. For gas jets in liquids, only the radial inflow velocities in the liquid will be measured, in order to evaluate entrainment properties of the flow.

The arrangement of the LDA is similar to the air jet tests. A single-channel, frequency-shifted configuration is used, with various beam orientations to measure velocity components. The optical axis of the sending optics is horizontal and parallel to the short side of the tank -- at its center. The measuring volume is viewed in the vertical direction, from a window set into the upper surface of the liquid. Natural seeding in the water is sufficient for operation of the system. Data acquisition and processing are indentical to the air jet study.

Void Fraction Distribution. The distribution of void fraction is a key observable for gas jets in liquids. This will be measured using the gamma ray absorption system illustrated in Fig. 10. This system will be assembled during the next phase of the work; therefore, only the planned arrangement is discussed in the following.

The radiation absorption system will be similar to Ohba (1976). A collimated gamma-ray beam of 59.6 KEV energy will be used, emitted from the artificial radiosotope $_{95}AM^{241}$, with a beam diameter of 10mm. This source is very stable with a half-life of roughly 400 years. Radiation from the beam will be detected using a scintillator counter consisting of a thallium activated sodium scintillator and a photomultiplier. The window of the detector will have a diameter of 1.5 mm -- providing reasonable spatial resolution for present conditions. The slit function of the detector will be deconvoluted, if necessary, to improve the spatial resolution. The linear absorption coefficient of gamma-ray radiation in water is

$24.2m^{-1}$, while it is about four orders of magnitude smaller for air; therefore, this radiosotope provides reasonably good sensitivity for present experimental conditions. Use of a relatively small aperture results in relatively low counting rates; therefore, times of counting will be on the order of 1-2 minutes for each path in order to obtain good signal-to-noise ratios. Background radiation will be eliminated using a pulse-height analyzer, similar to Ohba (1979). Shielding and safety requirements for this radiation source are minimal.

3.3 Theoretical Methods

The theoretical approach for water jets in water is the same as for air jets in air, described in Section 2.3. The analysis is also the same for subsonic air jets in water, under the LHF approximation, except that state relationships must be constructed for the air/water mixture. This is a straightforward process, c.f., Faeth (1983) or Sun (1985) for details. Calculations to this level are sufficient for the initial stages of the present investigation. The interesting problem of the interaction between shock waves and the liquid surface will be addressed, once methods have been established for underexpanded air jets in air.

3.4 Results and Discussion

During this report period, the test apparatus was designed, fabricated, and finally assembled at the Gas Dynamics Laboratories of the University of Michigan. Preliminary injector development tests were also undertaken using the smaller test apparatus of Sun (1984). Results obtained during these tests will be discussed in the following.

The arrangement for the preliminary tests involved a smaller windowed tank (410 mm x 534 mm x 913 mm high) with injection vertically upward in still water. Injectors of various types were used, fitted to the nozzle assembly used by Sun and Faeth (1985) and Sun et al. (1985). Nozzle exit diameters were 4-8 mm which is roughly half scale for the tests to be conducted using the new apparatus.

The appearance of a subsonic air jet in water for reasonably stable operation is illustrated in Fig. 11. This configuration involved a screen at the exit and a baffle to minize the disturbance of bubbles leaving the surface of the liquid. The nozzle shown in Fig. 11 also has a sharp lip, but this is not a necessary feature of a stable injector. The jet exit Reynolds number is reasonably high for the conditions shown in Fig. 11, ca. 10^4.

Bubbles are present near the edge of the jet for the flow pictured in Fig. 11. Drops are also probably present in the interior of the flow, however, we have no direct evidence of this. An interesting feature of the photograph is that the gas/liquid interface is more-or-less contiguous for the region shown. Farther downstream, the flow breaks up into a dispersed flow of bubbles. Even in the region shown, however, the interface is irregular and its geometry is clearly influenced by turbulence.

When the jet exit flow is underexpanded, the initial spread rate of the flow, indicated by the location of the interface, is increased. The surface is also disturbed with a finer-grain irregularity than that shown in Fig. 11. The more rapid spread is expected from the underexpanded gas jet results, c.f., Figs. 7-8. The higher Reynolds numbers are also expected to yield smaller scale disturbances. The tests showed, however, that near-injector interface location should be a useful observable for underexpanded gas jets in liquids.

Underexpanded gas jets are often used for injection in liquids to minimize effects of unstable flow with liquid slugging into the passage, e.g., the higher pressure gradient at the

Figure 11. Photograph of an air jet in water for stable operation.

exit forces liquid away from the passage. Unstable operation was observed during present tests for subsonic jets, with no screen at the passage exit and no baffle to reduce disturbances of bubble release at the liquid surface.

The appearance of the flow for unstable operation is illustrated in Fig. 32. In the cases shown, evidence of liquid slugging is seen by bubbles actually below the exit plane of the passage exit. In some photographs, the gas-containing region near the exit was completely severed by liquid as well. These conditions are also accompanied by an appreciable increase in noise generated by the flow. The screen and the baffle, or operation with relatively high levels of underexpansion, were required to eliminate these symptoms.

3.5 Summary

The gas-jet-in-water apparatus was assembled. Preliminary tests of injector operation were conducted in a subscale apparatus. Test results showed that liquid slugging could be controlled, even for subsonic jets, by placing a screen across the jet exit and by installing a baffle near the liquid surface. For stable jets, the liquid/gas interface is contiguous near the jet exit, with a bubble cloud adjacent to it. It is likely that drops are present on the gas side of the flow as well. The location of the interface near the jet exit is influenced by the degree of underexpansion of the flow and should be a useful observable.

Analysis of liquid/liquid and subsonic gas/liquid jets involves only cosmetic modifications of the analysis used for subsonic air jets in air. This analysis has been implemented on the University of Michigan computer system in preparation for upcoming evaluation tests.

The next phase of experimental work will involve structure (LDA) measurements for a water jet in water, as a baseline, and flow visualization tests for air injection in water. The gamma ray absorption instrument will also be developed and used to obtain void fraction distributions during gas injection into water.

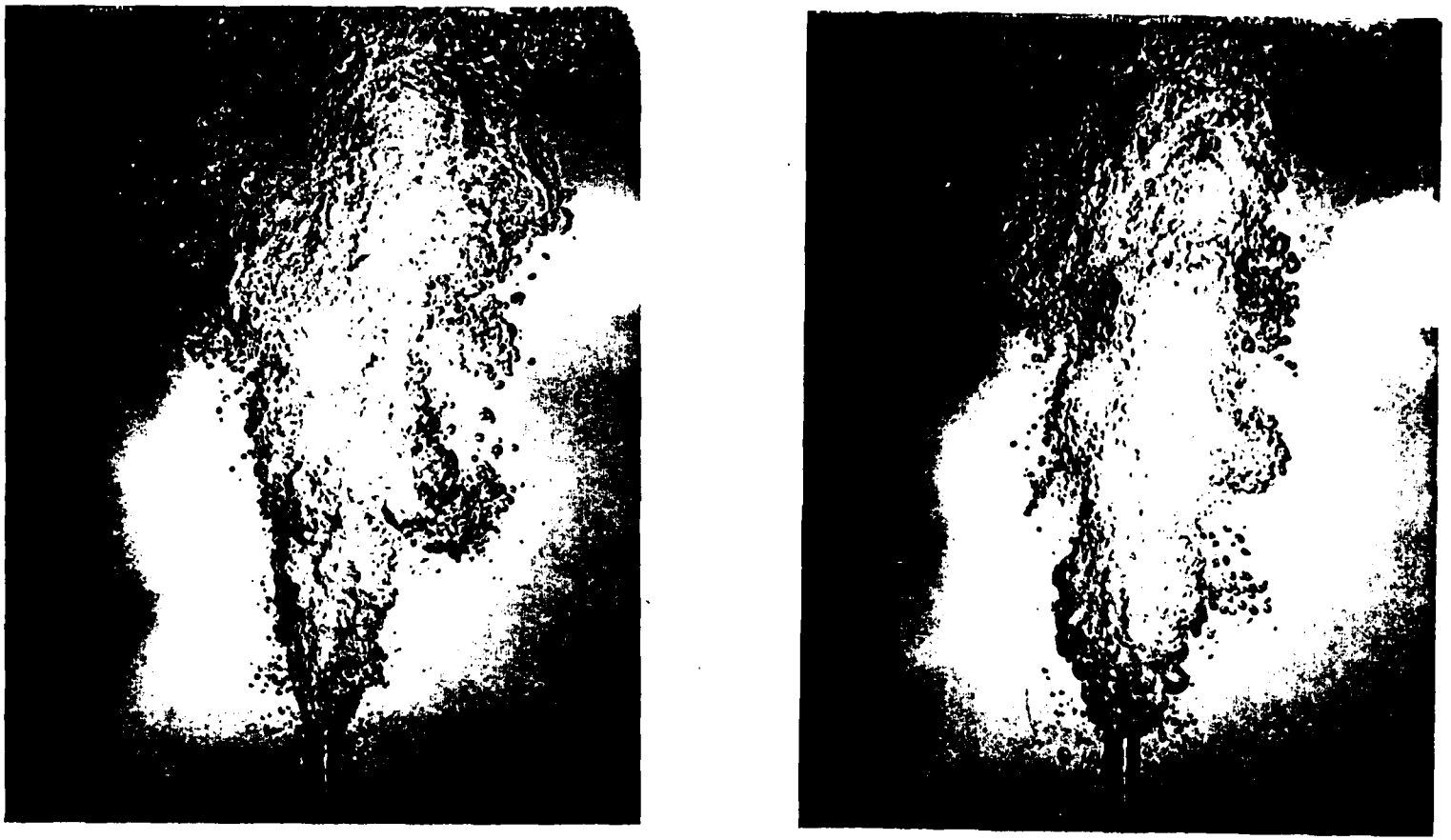

Figure 12. Photographs of an air jet in water for unstable operation.

REFERENCES

Abdel-Aal, H. K., Stiles, G. B. & Holland, C. C. 1966 Formation of interfacial area at high rates of gas flow through submerged orifices. AICHE J. 12, 174-180.

Addy, A. L. 1981 Effects of axisymmetric sonic nozzle geometry on Mach disk characteristics. AIAA J. 19, 121-122.

Al Taweel, A. M. & Landau, J. 1977 Turbulence modulation in two-phase jets. Int. J. Multiphase Flow 3, 341-351.

Avery, J. F. & Faeth, G. M. 1975 Combustion of a submerged gaseous oxidizer jet in a liquid metal. Fifteenth Symposium (International) on Combustion, The Combustion Institute, Pittsburgh, 419-428.

Bakaklevskii, Y. I. & Chekhovich, V. Y. 1978 Temperature field of a submerged steam jet, J. Engr. Phys. 34, 329-333.

Berman, H. A., Anderson, J. D., Jr. & Drummond, J. P. 1983 Supersonic flow over a rearward facing step with transverse nonreacting hydrogen injection. AIAA J. 21, 1707-1713.

Bilger, R. W. 1976 Turbulent jet diffusion flames. Prog. Energy Combust. Sci. 1, 87-109.

Birch, S. F. & Eggers, J. M. 1973 A critical review of the experimental data for developed free turbulent shear layers. Free Turbulent Shear Layers 1, NASA SP 321, 11-40.

Brankovic, A., Currie, I. G. & Martin, W. W. 1984 Laser-Doppler measurements of bubble plumes. Phys. Fluids 27 (2), 348-355.

Bush, K. L. & Merrill, G. L. 1981 SCEPS-an advanced thermal power plant for torpedoes. AIAA Paper No. 81-1602.

Chan, C. K. 1974 Dynamical pressure pulse in steam jet condensation. Proc. Fifth Intl. Heat Trans. Conf. 3, 226-230, ASME, New York.

Chen, L-D. & Faeth, G. M. 1982 Condensation of submerged vapor jets in subcooled liquids. J. Heat Transfer 104, 774-780.

Chen, L-D. & Faeth, G. M. 1983 Structure of turbulent reacting gas jets submerged in liquid metals. Comb. Sci. Tech. 31, 277-296.

Chesters, A. K. vanDoorn, M. & Goosens, L.J.H. 1980 A general model of unconfined bubble plumes from an extended source. Int. J. Multiphase Flow 6, 499-521.

Chun, J.-H. & Sonin, A. A. 1984 Small-scale simulation of vapor discharges into subcooled liquid pools. National Heat Transfer Conference, Niagara Falls, NY.

Cumo, M. Farello, G. E. & Ferrari, G. 1978 Direct heat transfer in pressure-suppression systems, Proc. Sixth Intl. Heat Trans. Conf., ASME, New York, 5, 101-106.

Dash, S. M., Wolf, D. E. & Seiner, J. M. 1985 Analysis of turbulent underexpanded jets, part II: parabolized Navier-Stokes model, SCIPVIS. AIAA J. 23, 505-514.

Drummond, J. P. & Weidner, E. H. 1982 Numerical study of a scramjet engine flowfield. AIAA J. 20, 1182-1187.

Edwards, R. V. & Jensen, S. V. 1983 Particle-sampling statistics in laser anemometers: sample-and-hold systems and saturable systems. J. Fluid Mech. 133, 397-411.

Eggers, J. M. 1966 Velocity profiles and eddy viscosity distributions downstream of a Mach 2.22 nozzle exhausting to quiescent air. NASA TN D-3601.

Faeth, G. M. 1983 Evaporation and combustion of sprays. Prog. Energy Combust. Sci. 9, 1-76.

Flack, R. D., Jr. & Thompson, H. D. 1977 Some laser velocimeter measurements in the turbulent wake of a supersonic jet. AIAA J. 15, 1507-1509.

Goldschmidt, V. W., Householder, M. K. & Chuang, S. C. 1971 Turbulent diffusion of small particles suspended in turbulent jets. Progress in Heat and Mass Transfer 6, Pergamon Press, Oxford, 487-508.

Groff, E. G. & Faeth, G. M. 1978 Phase equilibria in the Li-LiF-Li_2S system. Ind. Engr. Chem. Fundam. 17, 326-330.

Groff, E. G. & Faeth, G. M. 1978a A steady metal combustor as a closed thermal energy source. J. Hydronautics 12, 63-70.

Hughes, T. G., Smith, R. B. & Kiely, D. H. 1981 A stored chemical energy propulsion system (SCEPS) for underwater applications: its development and future. AIAA Paper No. 81-1601.

Jeng, S.-M. and Faeth, G.M. 1984 Species concentrations and turbulence properties in buoyant methane diffusion flames J. Heat Transfer 106, 721-727.

Kerney, P. J., Faeth, G. M. & Olson, D. R. 1972 Penetration characteristics of a submerged steam jet. AIChE J. 18, 548-553.

Kudo, A., Egusa, T. & Toda, S. 1974 Basic study on vapor suppression. Procl. Fifth Intl Heat Trans. Conf., ASME, New York, 3, 221-225.

Lai, M.-C., Jeng, S.-M. & Faeth, G. M. 1985 Structure of turbulent adiabatic wall plumes. Heat Transfer in Fire and Combustion Systems (Law, C. K., Jaluria, Y., Yuen, W. W. & Mijasaka, K., ed.), HTD-Vol. 45, ASME, New York, 181-190.

Lee, L., Bankoff, S. G. Yuen, M. C. & Tankin, R. S. 1979 Local condensation rate in horizontal co-current steam-water flow. 18th National Heat Transfer Conference, San Diego.

Lockwood, F. C. & Naguib, A. S. 1975 The prediction of the fluctuations in the properties of free, round jet, turbulent diffusion flames. Combustion and Flame 24, 109-124.

MacCormack, R. W. 1982 Numerical solution of compressible viscous flows. Ann. Rev. Fluid Mech. 11, 289-316.

McDaniel, J. C., Baganoff, D. & Byer, R. L. 1982 Density measurement in compressible flows using off-resonant laser-induced fluorescence. Phys. Fluids 25, 1105-1107.

Mahalingen, R., Limaye, R. S. & Brink, J. A., Jr. 1976 Velocity measurements in two-phase bubble-flow regime with laser-Doppler anemometry. AIChE. 22, 1152-1155.

Mao, C-P., Szekely, G. A., Jr. & Faeth, G. M. 1980 Evaluation of a locally homogeneous flow model of spray combustion. J. of Energy 4, 78-87.

Mikhail, A. G., Hankey, W. L. & Shang, J. S. 1980 Computation of a supersonic flow past an axisymmetric nozzle boat-tail with jet exhaust. AIAA J. 18, 869-875.

Milgram, J. H. 1983 Mean flow in round bubble plumes. J. Fluid Mech. 133, 345-376.

Ohba, K., Kishimoto, I. & Ogasawara, M. 1977 Simultaneous measurements of local liquid velocity and void fraction in bubbly flows using a gas laser--I. principles and measuring procedure. Tech. Rept. Osaka University 26, 547-556.

Ohba, K. 1979 Relationship between radiation transmissivity and void fraction in two-phase/dispersed flow. Ibid. 29, 245-254.

Robinson, C. E., Roux, J. A. & Bertrand W. T. 1979 Infrared measurements in an exhaust plume from an axisymmetric afterbody model at transonic Mach numbers. AEDC-TR-78-55.

Santoro, R. J., Semerjian, H. R., Emmerman, P. J. & Goulard, R. 1981 Optical tomography for flow field diagnostics. Int. J. Heat Mass Trans. 24, 1139-1150.

Schrock, V. E. 1969 Two-Phase Flow Instrumentation. ASME, New York, 24-35.

Seiner, J. M., Dash, S. M. & Wolf, D. E. 1985 Analysis of turbulent underexpanded jets, part II: shock noise features using SCIPVIS. AIAA J. 23, 669-677.

Serizawa, A., Kataoka, I. & Michiyoshi, I. 1975 Turbulence structure of air-water bubbly flow--II. local properties. Int. J. Multiphase Flow 2, 235-246.

Shearer, A. J., Tamura, H. & Faeth, G. M. 1979 Evaluation of a locally homogeneous flow model of spray evaporation. J. of Energy 3, 271-278.

Shuen, J.-S., Chen, L.-D. & Faeth, G. M. 1983a Evaluation of a stochastic model of particle dispersion in a turbulent round jet. AIChE J. 29, 167-170.

Shuen, J.-S., Chen, L.-D. & Faeth, G. M. 1983b Predictions of the structure of turbulent, particle-laden, round jet. AIAA J. 21, 1480-1483.

Shuen, J.-S., Solomon, A.S.P., Zhang, Q-F. & Faeth, G. M. 1984 Structure of particle-laden jets: measurements and predictions. AIAA J. 23, 396-404.

Simpson, M. E. & Chan, C. K. 1982 Hydrodynamics of a subsonic vapor jet in a subcooled liquid. J. Heat Trans. 104, 271-278.

Sindir, M. M. & Harsha, P. T. 1984 Turbulent transport models for scramjet flowfields. NASA CR-17284.

Solomon, A.S.P., Shuen, J-S., Zhang, Q-F. & Faeth, G. M. 1984a Structure of nonevaporating sprays: I. near-injector conditions and mean properties; II. drop and turbulence properties. AIAA _., in press.

Solomon, A.S.P., Shuen, J-S., Zhang, Q-F. & Faeth, G. M. 1984b Measurements and predictions of the structure of evaporating sprays. J. Heat Transfer 107, 679-686.

Soo, S. L. 1967 Fluid Dynamics of Multiphase Systems. Blaisdell Publishing Co., Waltham, MA.

Spalding, D. B. 1977 GENMIX: A General Computer Program for Two-Dimensional Parabolic Phenomena. Pergamon Press, Oxford.

Stanford, L. E. & Webster, C. C. 1975 Energy suppression and fission product transport in pressure-suppression pools. ORN-TM-3448.

Sun, T.-Y. 1985 A theoretical and experimental study of noncondensible turbulent bubbly jets. Ph.D. Thesis, The Pennsylvania State University, University Park, PA .

Sun, T.-Y. & Faeth, G. M. 1985 Structure of turbulent bubbly jets--I. methods and centerline properties;--II. phase property profiles. Int. J. Multiphase Flow, in press.

Sun, T.-Y., Parthasarathy, R. N. & Faeth, G. M. 1985a Structure of bubbly round condensing jets. Multiphase Flow and Heat Transfer (Dhir, V. K., Chen, J. C. & Jones, O. C. ed.), HTD-Vol. 47, ASME, New York, 75-84.

Sun, T.-Y., Parthasarathy, R. N. & Faeth, G. M. 1985b Bubbly condensing jets--I. methods and near-source properties;--II. mean and turbulent structure. J. Heat Transfer, submitted.

Tross, S. R. 1976 Characteristics of a turbulent two-phase, submerged, free jet. M.S. Thesis, The Pennsylvania State University, University Park, PA.

Wallis, G. 1969 One-Dimensional Two-Phase Flow. McGraw-Hill, New York.

Weimer, J. C., Faeth, G. M. & Olson, D. R. 1973 Penetration of vapor jets submerged in subcooled liquids. AIChE J. 19, 552-558.

Vatsa, V. N., Werle, M. J. & Anderson, O. L. 1981 Solution of slightly underexpanded two-dimensional and axisymmetric coflowing jets. AIAA J. 19, 303-310.

Vatsa, V. N., Werle, M. J., Anderson, O. L. & Hankins, G. B. 1982 Solutions for three-dimensional over- or underexpanded exhaust plumes AIAA J. 20, 1188-1194.

Young, R. J., Yang, K. T. & Novotny, J. L. 1974 Vapor-liquid interaction in a high velocity vapor jet condensing in a coaxial water flow. Proc. Fifth Intl. Heat Trans. Conf. 3, ASME, New York, 226-230.

END

FILMED

11-85

DTIC